

# Sphaleron and gravitational wave with the Higgs-Dilaton potential in the Standard Model Two-Time Physics

Vo Quoc Phong<sup>a,b,\*</sup>, Quach Ai Mi<sup>a,b,†</sup> and Nguyen Xuan Vinh<sup>a,b,‡</sup>

<sup>a</sup>*Department of Theoretical Physics, University of Science, Ho Chi Minh City 700000, Vietnam*

<sup>b</sup>*Vietnam National University, Ho Chi Minh City 700000, Vietnam*

By introducing a Higgs-Dilaton potential, the 2T model has full triggering for a first order electroweak phase transition, namely for the mass of Dilaton between 300 GeV and 550 GeV. We have also compared the transition strengths in the case with and without daisy loops, the difference being always less than 0.2. The effective Higgs potential has given a sphaleron energy less than 8.4 TeV. The value of  $\beta/H^*$  is larger than 25 and less than 34 in all cases that are sufficient to trigger the first order electroweak phase transition. Gravitational wave energy density caused by this transition, may be sufficiently detected by future detectors, could indirectly confirm Dilaton.

Keywords: Spontaneous breaking of gauge symmetries, Extensions of electroweak Higgs sector, Particle-theory models (Early Universe)

## I. INTRODUCTION

Multidimensional theories have become an important phenomenological research framework. However, from 2008, besides the string theory, the multi-dimensional model that fully combines with particle physics is currently only the 2T theory [1–7]. The one not only provides us with a new view of time but also proposes new mechanisms for difficult problems. The cause of them may be from an exotic particle in the 2T model, Dilaton.

The 2T model is a form of space-time extension but at the same time proposes a new particle, Dilaton which is originally a candidate for Axion. However, the role of Dilaton

---

\*Electronic address: vqphong@hcmus.edu.vn

†Electronic address: aimiwu14498@gmail.com

‡Electronic address: vinhnguyen.mxt@gmail.com

could be more numerous. It as previously investigated is a source of strong CP violation and is likely also responsible for current difficult physics problems.

The first order electroweak phase transition (EWPT) problem was solved in the 2T elementary particle model. According to current research, the triggers can be Dark matter (DM) or new heavy bosons Refs. [8–34]. As in the studies of other authors, the cause of first order phase transition is due to the dominant activation of Dilaton which is stored in an external potential of Dilaton.

Dilaton is a fairly common name. The concept of Dilaton also appears in many other theories, for example in The Composite Higgs models. However, Dilaton in the 2T model is a particle associated with the concept of two time dimensions and the symmetry  $SP(2, R)$ .

At present, the evidence for extra dimensions is very weak. Instead of looking for it, the 2T model needs to be enabled and look for the evidence of Dilaton. This also indirectly proves the existence of extra dimensions. The electroweak phase transition may be the clue for this search. Because the problem can give us the possible mass domain of Dilaton, sketching a form of Dilaton potential. In addition, it makes clearer the mass generation scenario for particles.

In Ref.[35], we proposed a form of Dilaton potential with the non-zero mass Dilaton which is sufficient to trigger a first order electroweak phase transition. However, in Ref.[35] with a one-loop effective potential without daisy loops, the necessary mass domain for Dilaton is given but not completely. In this paper, an effective potential with daisy loops is used to recalculate more accurately the phase transition strength ( $S$ ) and other quantities in the Baryogenesis scenario. Specifically the sphaleron energy and the gravitational wave energy (GW) density are calculated.

This article is organized as follows. In section II, the types of Dilaton potentials are discussed again. Then the strength of EWPT is calculated in the case of a one-loop effective potential with Daisy loops. The comparison of phase transition strength in the case with and without daisy loops. In section III, by using static fields and spherically symmetric bubble nucleations, sphaleron energy and gravitational waves are solved numerically with a wide range of Dilaton mass. We make a general assessment of sphaleron energies, comparing the gravitational wave energy density with current data. Finally, we summarize and make outlooks in section IV, such as evaluating the compatibility of sphaleron with other conditions and giving a way to search for an first order electroweak phase transition.

## II. CONTROLLING EWPT BY THE HIGGS-DILATON POTENTIAL

The basic concepts as well as the 2T elementary particle model of 2T theory were built by I. Bars [5] when considering multidimensional concepts. In our opinion, it is like an extension of the concept of time. This model has successes such as solving the problem of strong CP violation, providing DM candidates [3].

The SM in the 2T model includes the Higgs scalar fields  $H$  and Dilaton  $\Phi$ , the left/right chiral fermion fields  $\Psi^L, \Psi^R$  (which are quarks and leptons), and the gauge bosons  $A_M$  that accompany the gauge symmetry of this model [5].

With the  $SP(2, R)$  symmetry, the Higgs-Dilaton potential [6] has the following form,

$$V(\Phi, H) = \lambda (H^\dagger H - \alpha^2 \Phi^2)^2 + V(\Phi),$$

in which  $\lambda, \alpha$  are dimensionless couplings.  $H$  and  $\Phi$  are the  $SU(2)$  Higgs and Dilaton doublet respectively. Initially  $V(\Phi)$  had no specific form. But it is the key to examining EWPT and related quantities [36]. The minimization process Eq. (II) leads to the Higgs and Dilaton fields having non-zero VEV and being linearly proportional to each other [5, 35].

After reducing to 1T, we get the 4D Higgs-Dilaton potential as follows:

$$V(h, \phi) = \lambda [\chi^2 - \alpha^2 \phi^2]^2 + V(\phi), \chi(x) = \frac{1}{\sqrt{2}}(v + h(x)), \phi = \frac{1}{\alpha\sqrt{2}}(v + \alpha d(x)), \quad (1)$$

in which  $v = 246$  GeV,  $h, d$  scalar fields with zero VEVs. When  $v(\phi)$  is involved,  $h, d$  are not physical fields yet. Because  $V(h, \phi)$  will contain mixed components between  $h$  and  $d$ . Depending on the form of  $V(\Phi)$ , the diagonalization process will yield physical particles.

The potential  $V(\Phi)$  must be of the form  $\Phi^4$  to ensure the symmetry  $SP(2, R)$ . However, in general this potential can be extended if we accept a soft breaking of the symmetry  $SP(2, R)$ . As in Ref.[35],  $V(\Phi) \sim const.\Phi^4 + const.\Phi^2$  has been assumed.

The form of  $V(\Phi)$  is still under consideration in some cases, for example in connection with gravity. In Table I the choices of  $V(\Phi)$  are summarized.

The Dilaton field in the 2T model with a potential of only order 4, is like a degree of freedom or it has near zero mass but has a non-zero VEV.

So this is something different from SM. However, the electroweak symmetry breaking is accompanied by the  $SP(2, R)$  symmetry breaking. When this symmetry is broken, the Dilaton potential is no longer only of order 4. This can be explained mathematically by choosing the function  $f(\mathcal{S}/\Phi)$ .

$f(\mathcal{S}/\Phi)$	$V(H, \Phi)$	$\mathcal{S}$	$V(\Phi)$	Refs.
$V(H, \Phi) = f(s/\Phi)\Phi^4$				
$\frac{\lambda}{4}(\mathcal{S}^2/\Phi^2 - \alpha^2)^2 + \rho/4$	$\lambda(H^\dagger H - \alpha^2\Phi^2)^2 + \rho\Phi^4$	$\sqrt{2H^\dagger H}$	$\rho\Phi^4$	Refs.[36]
$\frac{\lambda}{4}(\mathcal{S}^2/\Phi^2 - \alpha^2)^2 + \rho/4 + \frac{\omega^2}{\kappa^2\Phi^2}$	$\lambda(H^\dagger H - \alpha^2\Phi^2)^2 + \rho\Phi^4 + \frac{\omega^2}{\kappa^2}\Phi^2$	$\sqrt{2H^\dagger H}$	$\rho\Phi^4 + \frac{\omega^2}{\kappa^2}\Phi^2$	Refs.[35, 36]

TABLE I: Cases of the Higgs-Dilaton potential

### A. The Dilaton potential

In this study, an added Dilaton potential has the following form [35]:

$$V(\Phi) = \rho\Phi^4 - \frac{\omega^2}{\kappa^2}\Phi^2. \quad (2)$$

$\omega$  is much smaller than  $\kappa$ . Let the second term in Eq.2 be a soft-breaking component of the  $SP(2, R)$  symmetry. In general, we can choose  $\kappa$  to be arbitrarily large, so the above inequality can always be satisfied.

$$V(\phi) = \frac{\rho}{\kappa^4}\phi^4 - \frac{\omega^2}{\kappa^4}\phi^2. \quad (3)$$

This assumption could be justified if one takes into account the next leading order of 2T metric in the action [5] and  $Z_2$  symmetry of Dilaton.  $\kappa^4$  will be simplified by the 2T action when reduced to 1T [5]. Then by substituting the above Higgs and Dilaton fields into the Higgs-Dilaton potential, the potential is rewritten in terms of the variable  $\phi_c$  which is a re-notation of VEV,

$$\begin{aligned} V(h, \phi) &= \frac{\lambda}{4} [(\phi_c + h)^2 - (\phi_c + \alpha d)^2]^2 - \frac{\omega^2}{2\alpha^2}(\phi_c + \alpha d)^2 + \frac{\rho}{4\alpha^4}(\phi_c + \alpha d)^4 \\ &= \left\{ \left( \frac{\rho}{4\alpha^4}\phi_c^4 - \frac{\omega^2}{2\alpha^2}\phi_c^2 \right) + \left( \frac{\rho}{\alpha^3}\phi_c^3 - \frac{\omega^2}{\alpha}\phi_c \right) d \right. \\ &\quad \left. - 2\lambda\alpha\phi_c^2hd + \lambda\phi_c^2h^2 + \left( \lambda\alpha^2\phi_c^2 - \frac{\omega^2}{2} + \frac{3\rho}{2\alpha^2}\phi_c^2 \right) d^2 \right\} + \text{interaction terms}, \quad (4) \end{aligned}$$

Eq.(4) appears the term  $hd$  so they are not physical particles yet. In the 2T spacetime, the  $\omega^2/\kappa^2\Phi^2$  component will be so small that it can be neglected. However, when reducing the spacetime to 1T, the  $\kappa^4$  parameter in Eq.(3) is lost, so the  $\omega^2\phi^2$  component can have a significant contribution and lead to a Dilaton with non-zero mass.

After diagonalization, we obtain physical particles which have masses at tree level as [35]

$$m_{d'}^2 = \frac{2\alpha^4\lambda\phi_c^2 + 2\alpha^2\lambda\phi_c^2 + 3\rho\phi_c^2 - \alpha^2\omega^2}{2\alpha^2} - \frac{\sqrt{8\alpha^2\lambda\phi_c^2(\alpha^2\omega^2 - 3\rho\phi_c^2) + (\phi_c^2(2\alpha^4\lambda + 2\alpha^2\lambda + 3\rho) - \alpha^2\omega^2)^2}}{2\alpha^2}, \quad (5)$$

$$m_{h'}^2 = \frac{2\alpha^4\lambda\phi_c^2 + 2\alpha^2\lambda\phi_c^2 - \alpha^2\omega^2 + 3\rho\phi_c^2}{2\alpha^2} + \frac{\sqrt{8\alpha^2\lambda\phi_c^2(\alpha^2\omega^2 - 3\rho\phi_c^2) + (\phi_c^2(2\alpha^4\lambda + 2\alpha^2\lambda + 3\rho) - \alpha^2\omega^2)^2}}{2\alpha^2}. \quad (6)$$

In Eq. (5), as  $\omega$  and  $\rho$  go to zero,  $m_d^2 = 0$ , which is in agreement with the results in Ref. [5]. The above formulas can be rewritten as follows

$$m_{h'}^2(\phi_c) = A\phi_c^2, \quad (7)$$

$$m_{d'}^2(\phi_c) = B\phi_c^2, \quad (8)$$

here  $A, B$  are the parameters. For convenience,  $h', d'$  will be denoted again as  $h, d$  in the following sections. The contribution of extra dimensions does not only appear in one effective potential via Dilaton but also in the mass of Higgs and other fields as well.

Thus, Dilaton has a very interesting property, the manifestation of Dilaton in 1T spacetime is a massless particle. Or in other words, the manifestation of 6-dimensional spacetime (2T spacetime) is through the mass of Dilaton.

Furthermore, from the 2T sectors reduced to 1T, analyzed and diagonalized, the masses of gauge fields are obtained [3, 5],

$$m_t^2(\phi_c) = \frac{h_t^2}{2}\phi_c^2 = \frac{m_t^2}{v^2}\phi_c^2, \quad (9)$$

$$m_W^2(\phi_c) = \frac{g_1^2}{4}\phi_c^2 = \frac{m_W^2}{v^2}\phi_c^2, \quad (10)$$

$$m_Z^2(\phi_c) = \frac{g_1^2 + g_2^2}{4}\phi_c^2 = \frac{m_Z^2}{v^2}\phi_c^2, \quad (11)$$

where  $m_i \equiv m_i(v)$  is the mass of field  $i$  at 0K and  $v = 246$  GeV, is equal to VEV in SM. Here  $\phi_c$  is understood as VEV at temperature  $T$ . Therefore, the change from the symbol  $v$  to  $\phi_c$  in the previous steps is convenient for writing expressions at temperature  $T$ .

Therefore from Eq.(7) to Eq.(11), the full mass spectra of particles that make significant contributions to the effective potential.

## B. The effective potential and searching $S$

The mass generation mechanism for particles in this model is still through the Higgs field like SM, however the Higgs field is always accompanied by the Dilaton field since the creation of non-zero VEV of the Higgs field requires a Dilaton field. This process is clearly shown in the minimization of the Higgs-Dilaton potential [2–7, 35].

The effective one-loop potential is usually calculated in the manner of Jackiw [37–39] which is developed from the Coleman-Weinberg potential. The effective one-loop potential at 0K can be written as

$$V_{\text{eff}}^{0K}(\phi_c) = \frac{\lambda_R}{4}\phi_c^4 - \frac{m_R^2}{2}\phi_c^2 + \Lambda_R + \frac{1}{64\pi^2} \sum_{i=h,d,W,Z,t} n_i m_i^4(\phi_c) \ln \frac{m_i^2(\phi_c)}{v^2},$$

where  $\lambda_R, m_R, \Omega_R$  are renormalized parameters,  $m_i(\phi_c)$  is mass at tree level derived in previous subsection, i.e., SM particles and Dilaton;  $n_i$  with  $i = d, h, W, Z, t$  are constants related to the degrees of freedom of each field and are given by

$$n_h = n_d = 1, n_W = 6, n_Z = 3, n_t = -12.$$

To work out renormalized parameters, the familiar normalization conditions will be used,

$$\begin{cases} V_{\text{eff}}(v) = 0, \\ V'_{\text{eff}}(v) = 0, \\ V''_{\text{eff}}(v) = m_h^2, \end{cases}$$

from which the coefficients in the effective potential are found out the following results

$$\begin{cases} \lambda_R = \frac{m_h^2}{2v^2} - \frac{1}{16\pi^2 v^4} \sum_i n_i m_i^4 \left( \ln \frac{m_i^2}{v^2} + \frac{3}{2} \right), \\ m_R^2 = \frac{m_h^2}{2} - \frac{1}{16\pi^2 v^2} \sum_i n_i m_i^4, \\ \Lambda_R = \frac{m_h^2 v^2}{8} - \frac{1}{128\pi^2} \sum_i n_i m_i^4. \end{cases}$$

In case the daisy loops are taken into account, at the high temperature, the effective potential takes the form,

$$V_{\text{eff}}(\phi_c, T) = \frac{\lambda(T)}{4}\phi_c^4 + D(T^2 - T_0^2)\phi_c^2 - \frac{T}{12\pi} \sum_{h,W,Z,d} g_i \left[ \frac{m_i^2 \phi_c^2}{v^2} + \Pi_i(T) \right]^{\frac{3}{2}}. \quad (12)$$

If we do not consider daisy loops, Eq.(12) will not have  $\Pi_i$  functions, the coefficients in Eq.(12) are of the form,

$$\lambda(T) = \frac{m_h^2}{2v^2} + \frac{1}{16\pi^2 v^4} \left( \sum_{i=h,d,W,Z} n_i m_i^4 \ln \frac{A_b T^2}{m_i^2} + n_t m_t^4 \ln \frac{A_f T^2}{m_t^2} \right),$$

$$D = \frac{m_h^2 + m_d^2 + 6m_W^2 + 3m_Z^2 + 6m_t^2}{24v^2}, \quad (13)$$

$$T_0^2 = \frac{1}{D} \left[ \frac{m_h^2}{4} - \frac{1}{32\pi^2 v^2} \sum_{i=h,d,W,Z,t} n_i m_i^4 \right].$$

The contributions of daisy loops are stored in the following functions,

$$\Pi_W(T) = \frac{22}{3} \frac{m_W^2}{v^2} T^2, \quad (14)$$

$$\Pi_Z(T) = \frac{22}{3} \frac{(m_Z^2 - m_W^2)}{v^2} T^2, \quad (15)$$

$$\Pi_h(T) = \frac{m_h^2 + 2m_W^2 + m_Z^2 + 2m_t^2}{4v^2} T^2, \quad (16)$$

$$\Pi_d(T) \sim \frac{m_d^2}{v^2} T^2. \quad (17)$$

In Eq.(12),  $\ln A_b = 3.907$  or  $\ln A_f = 1.135$ , and there is an additional contribution of Dilaton, which will push the EWPT process to be more intense. As analyzed in the case without daisy loops in Ref.[35],  $300 \text{ GeV} \leq m_d \leq 650 \text{ GeV}$ , it will have the large enough EWPT strength ( $S$ ). However, when the mass of Dilaton is too large, it will lead to large error in the effective potential. In Ref.[35] only  $s$  is calculated but the convergence conditions and errors of the effective potential are taken into account. If  $m/T$  is not less than 2.2 the potential difference will be in error by more than 5% [40].

$S = \frac{\phi_c}{T_c}$ , is the ratio of VEV to the temperature at the time of phase transition.  $T_c$  is called the critical temperature. With the equations from Eq.(12) to Eq.(16), we can probe  $S$  for any given mass of Dilaton.

The daisy loop contribution of Dilaton is ignored because its mass is larger than that of Top quark and at temperatures around 100 – 200 GeV its contribution is small. Also the exact calculation of these contributions is quite complicated, we can only estimate them as Eq.(17). The equations from (14) to (16), can be found in Refs.[41–43] for details, reduces the value of 3rd order component in Eq.(12), leading to  $S$  decreasing when there are daisy loops.

The first order EWPT will be detected again in this section and then calculate the sphaleron energy and gravitational wave in the next section.

The steps to find  $S$  are as follows:

- Choosing the Dilaton mass domain. Following Ref.[35], we choose the Dilaton mass from 300 GeV.
- Running the effective potential for different temperatures.  $T_c$  is the temperature for which  $v_{eff}(\phi_c, T_c) = 0$ .
- $\phi_c$  is the second non-zero VEV of  $v_{eff}$ . From there we calculate  $S = \frac{\phi}{T_c}$ . The convergence condition for  $\phi_c$  is that it must be less than 246 GeV.

The results as the first four columns in Table II. When the Dilaton mass is larger than 550 GeV,  $\phi_c$  does not converge to 246 GeV but exceeds 246 GeV.  $S$  with daisy loops is always smaller than one without daisy loops. However, this difference does not exceed 0.2 or 10%. This also further confirms that the contribution of daisy loops in the critical temperature region is negligible but their contributions become significant in the higher one.

$m_d$	$v_c$	$T_c$	$S$	$E$ [GeV]	$E_0$ [GeV]	$\alpha$	$\frac{\beta}{H_*}$	$\Omega h^2(f_{peak})$	Daisy loops
300	107.492	136.162	0.789439	7658.14	9106.11	0.00766406	25.3093	$6.34889 \times 10^{-16}$	with
	98.2028	146.281	0.671331	7636.04		0.00480408	23.4906	$1.08379 \times 10^{-16}$	without
350	133.417	129.726	1.02845	7751.48	9094.9	0.0132065	26.8886	$5.07648 \times 10^{-15}$	with
	128.617	138.449	0.928987	7727.12		0.00945377	25.1155	$1.46259 \times 10^{-15}$	without
400	160.455	122.702	1.30768	7905.02	9079.14	0.0211503	28.991	$2.958 \times 10^{-14}$	with
	158.371	130.329	1.21517	7888.4		0.0161664	27.2371	$1.10564 \times 10^{-14}$	without
450	190.502	115.103	1.65505	8113.7	9055.43	0.0326829	31.7208	$1.44943 \times 10^{-13}$	with
	189.376	121.835	1.55436	8106.3		0.0256766	29.9408	$6.06993 \times 10^{-14}$	without
500	229.877	108.027	2.12796	8392.06	9020.63	0.0522199	34.9581	$7.77137 \times 10^{-13}$	with
	227.515	113.854	1.99831	8384.29		0.0410284	33.1385	$3.30201 \times 10^{-13}$	without
550	287.102	106.276	2.70147	8792.76	8970.03	0.0938256	37.2308	$6.25938 \times 10^{-12}$	with
	281.168	110.832	2.53687	8769.76		0.0725315	35.6069	$2.57741 \times 10^{-12}$	without
600	348.246	114.415	3.04372	9264.72	8895.83	0.158098	36.4387	$3.90875 \times 10^{-11}$	with
	339.772	117.85	2.88309	9229		0.123424	35.2402	$1.73786 \times 10^{-11}$	without

TABLE II: Results in the cases of Dilaton.

### III. SPHALERON AND GRAVITATIONAL WAVE

Under the conditions of Baryogenesis, B violation must be mandatory and requires the existence of a sufficiently large sphaleron rate or sphaleron are relevant for the B violating processes.

The sphaleron energy functional consists of three components: the contribution of gauge fields, the Higgs kinetic energy and the effective potential.

$$E_{sph} = \int dx^3 \left[ \frac{1}{4} W_{ij}^a W_{ij}^a + (D_i \phi)^\dagger (D_i \phi) + V_{eff} \right]. \quad (18)$$

With the static field approximation (ie.,  $W_0^a = 0$ ) and sphaleron in the spherically symmetric form [44]:

$$\begin{cases} \phi(r) = \frac{v}{\sqrt{2}} h(r) i n_a \sigma \begin{pmatrix} 0 \\ 1 \end{pmatrix}, \\ W_i^a(r) = \frac{2}{g} \epsilon^{aij} n_j \frac{f(r)}{r}, \end{cases} \quad (19)$$

where  $n_i \equiv \frac{x^i}{r}$  and  $r$  is the radial coordinate in the spherical coordinates.

The non-zero temperature Sphaleron energy functional is written as follows

$$E_{sph}^T = \frac{4\pi v}{g} \int_0^\infty d\xi \left[ 4 \left( \frac{df}{\xi} \right)^2 + \frac{8f^2(1-f)^2}{\xi^2} + \frac{\xi^2}{2} \left( \frac{dh}{\xi} \right)^2 + h^2(1-f)^2 + \frac{\xi^2}{g^2 v^4} V_{eff}(h, T) \right], \quad (20)$$

in which  $g^2 = \frac{G_F 8m_W^2}{\sqrt{2}}$ ;  $G_F = 1.166 \times 10^{-5} \text{ GeV}^{-2}$ ;  $m_W = 80.39 \text{ GeV}$ ,  $\xi \equiv gvr$ .

Taking the variation of above function in terms of  $h$  and  $f$ , we will obtain the equations of motion,

$$\xi^2 \frac{d^2 f}{d\xi^2} = 2f(1-f)(1-2f) - \frac{\xi^2}{4} h^2(1-f), \quad (21)$$

$$\frac{d}{d\xi} \left( \xi^2 \frac{dh}{d\xi} \right) = 2h(1-f)^2 + \frac{\xi^2}{g^2 v^4} \frac{\partial V_{eff}}{\partial h}. \quad (22)$$

The contribution of effective potential to the sphaleron energy is less than 45%, but the effective potential acts as a source for bubbles (as seen from Eq.(21) and (22)).

Here,  $h(\xi)$  and  $f(\xi)$  have boundary conditions

$$\begin{cases} h(\xi \rightarrow 0) = f(\xi \rightarrow 0) = 0, \\ h(\xi \rightarrow \infty) = f(\xi \rightarrow \infty) = 1. \end{cases} \quad (23)$$

These boundary conditions ensure that the sphaleron energy converges, because from Eqs. (22), (21) and (20), as  $r$  increases, the functions  $f, h$  must approach 1 and the components in Eq.(20) must approach 0.

For equations from (20) to (23), the numerical solutions are obtained as Fig. 1 and Table II.

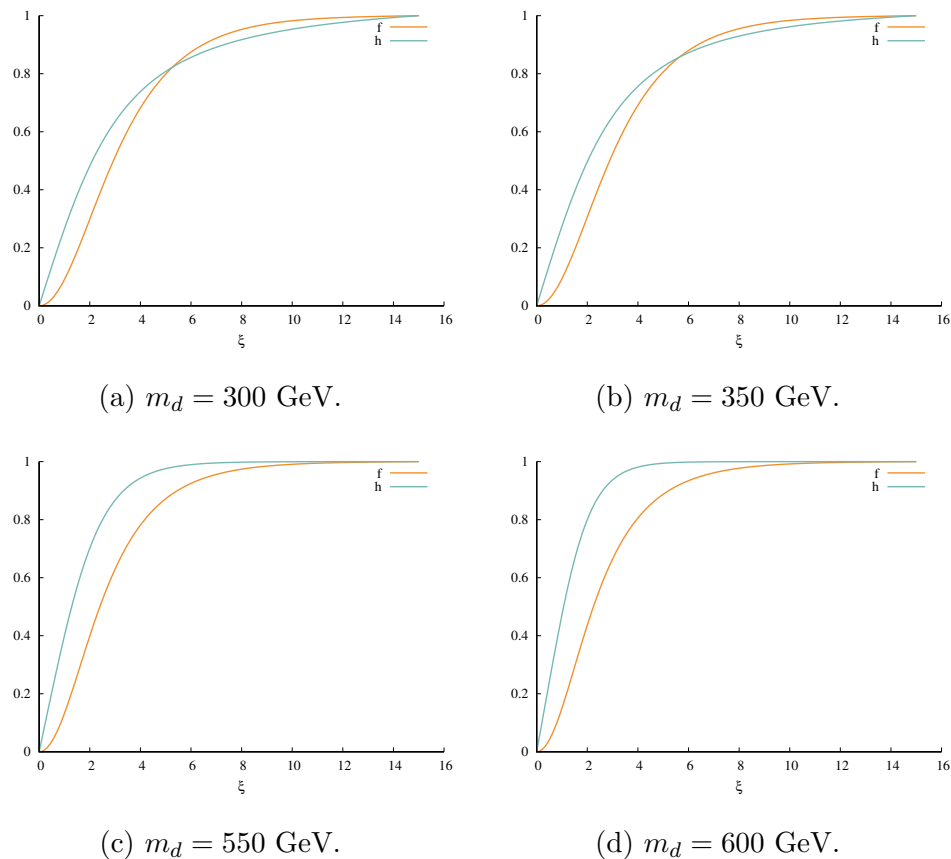


FIG. 1: Profile functions with the differential dilaton masses.

In Fig. 1, the larger the mass of Dilaton is, the faster  $f(r), h(r)$  approaches 1. This is consistent with the results in Table II, the larger the mass of Dilaton is, the larger  $S$  is. When  $m_d < 350$  GeV,  $f(r)$  approaches 1 faster than  $h(r)$  but when  $m_d > 350$  GeV this approach to 1 happens in reverse. Because the larger  $m_d$  is, the stronger the interaction between Higgs and Dilaton is, further delaying the expansion of Higgs bubble nucleation.

The largest sphaleron energy is about 9.2 TeV with the Dialton mass of about 600 GeV. But to avoid the VEV divergence problem, the Dilaton mass must be less than 550 GeV, the best sphaleron energy in this model is about 8.4 TeV. This energy range is about 1 TeV

smaller than that in the SM.

There are three processes which are involved in the production of GWs at a first-order PT: Collisions of bubble walls, sound waves in the plasma and Magnetohydrodynamic (MHD) turbulence [45]. These three processes generically coexist, and the corresponding contributions to the stochastic GW background should linearly combine, at least approximately, so that [45]

$$h^2\Omega_{GW} = h^2\Omega_{Coll} + h^2\Omega_{sw} + h^2\Omega_{tur}. \quad (24)$$

There are three different scenarios depending on the bubble wall velocity [45] which is defined via  $\alpha$ :

$$v_b = \frac{\frac{1}{\sqrt{3}} + \sqrt{\alpha^2 + \frac{2\alpha}{3}}}{1 + \alpha}. \quad (25)$$

We estimate that  $v_b \sim 1$ . This will be clearly seen on Table II. Therefore, the generation of gravitational waves has only two components: the sound wave and turbulence [45–51].

The gravitational wave energy density parameters of sound waves is defined as follows [45, 52]:

$$h^2\Omega_{sw}^2(f) = 2.65 \cdot 10^{-6} v_b k_w^2 \frac{H^*}{\beta} \left( \frac{\alpha}{1 + \alpha} \right)^2 \left( \frac{100}{106.75} \right)^{1/3} S_{sw}(f), \quad (26)$$

where

$$\begin{cases} S_{sw} = \left( \frac{f}{f_{peak,sw}} \right)^3 \left( \frac{7}{4+3\left(\frac{f}{f_{peak,sw}}\right)^2} \right)^{7/2} \\ v_b \sim 1. \\ k_w = \alpha(0.73 + 0.083\sqrt{\alpha} + \alpha)^{-1}. \end{cases} \quad (27)$$

And GWs from turbulence in the cosmic fluid is given by

$$h^2\Omega_{tur}^2(f) = 3.35 \cdot 10^{-4} \left( \frac{k_t \alpha}{1 + \alpha} \right)^{3/2} \frac{H^*}{\beta} \left( \frac{100}{106.75} \right)^{1/3} S_{tur}(f), \quad (28)$$

in which

$$\begin{cases} S_{tur} = \left( \frac{f}{f_{peak,tur}} \right)^3 \left( \frac{1}{1 + \left(\frac{f}{f_{peak,tur}}\right)} \right)^{11/3} \frac{1}{1+8\pi f/h^*} \\ h^* = \frac{16.5 \cdot 10^{-3} T_c}{100} \left( \frac{106.75}{100} \right)^{1/6} \\ v_b \sim 1. \\ k_t = 0.05\alpha(0.73 + 0.083\sqrt{\alpha} + \alpha)^{-1} \\ f_{peak,tur} = 2.7 \cdot 10^{-2} \frac{\beta}{H^*} \frac{T_c}{100} \left( \frac{106.75}{100} \right)^{1/6}. \end{cases} \quad (29)$$

Because the effective potential contributes about 45% to the sphaleron energy. We have a possible approximation [53],

$$\frac{\beta}{H^*} \approx \left[ T \frac{d(S(t))}{dT} \right]_{T=T_C} \approx \left[ T \frac{d(S_3/T)}{dT} \right]_{T=T_C} \approx \left[ T \frac{d\left(0.45 \frac{E_{sph}^T}{T}\right)}{dT} \right]_{T=T_C}. \quad (30)$$

The second parameter  $\alpha$  is determined at the nucleation temperature as follows [54–56]:

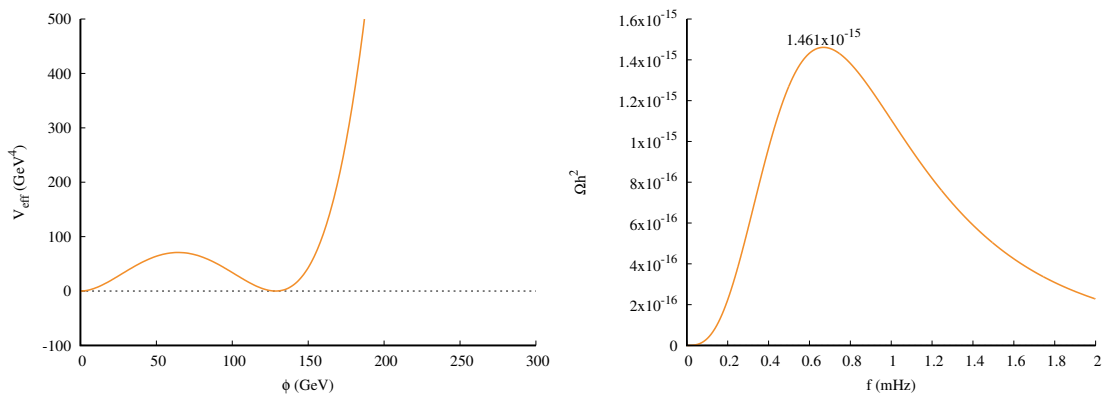
$$\alpha = \frac{\epsilon}{\rho_{rad}^*}, \quad (31)$$

$$\epsilon = \left( V_{eff}(v(T), T) - T \frac{d}{dT} V_{eff}(v(T), T) \right)_{T=T_C}, \quad (32)$$

$$\rho_{rad}^* = g^* \pi^2 \frac{T_c^4}{30} = 106.75 \pi^2 \frac{T_c^4}{30}. \quad (33)$$

This parameter depends only on the configuration of effective potential. Thus in all models the parameter which is easily calculated by usual way when the effective potential is known, determines the strength of phase transition.

From equations (26), (28) and related formulas, we solve numerically and obtain the results at  $T_* = T_c$  in Table II and Figs. 2, 3, 4.

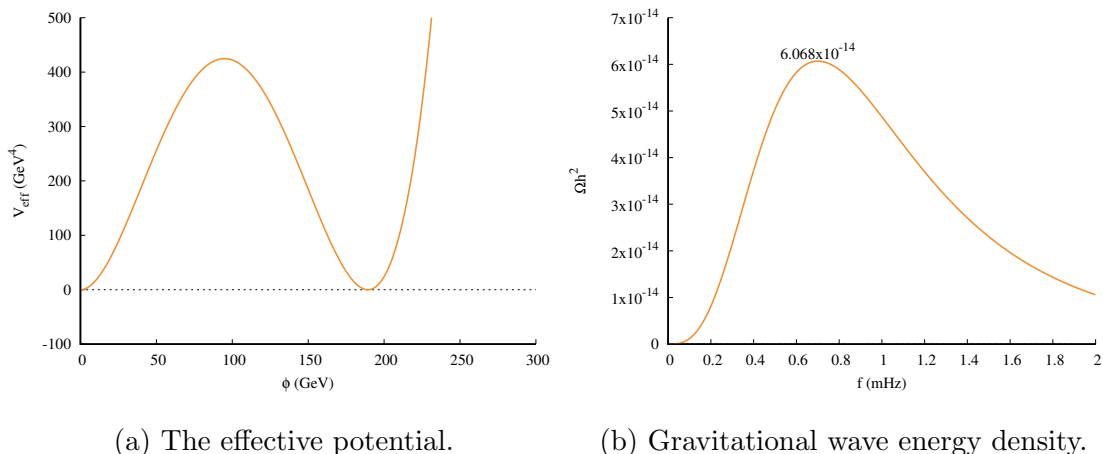


(a) The effective potential.

(b) Gravitational wave energy density.

FIG. 2: In the case of  $m_d = 350$  GeV.

In Fig.2 and 3, the larger  $m_d$  is, the higher the barrier of effective potential is, the higher the maximum of  $\Omega h^2$  is. Because the higher the barrier is, the more shocking the EWPT process is, so the gravitational waves generated from it are larger. Furthermore, for  $\Omega h^2$  to increase 10 times, the mass of Dilaton increases by 50 GeV.

FIG. 3: In the case of  $m_d = 450$  GeV.

In Fig. 4, for  $300 \text{ GeV} \leq m_d < 600 \text{ GeV}$ , the maximum value of  $\Omega h^2$  lies in the range from  $10^{-16}$  to  $10^{-11}$ . This is a very wide range, or in other words  $\Omega h^2$  increases very rapidly over a mass range of 300 GeV.

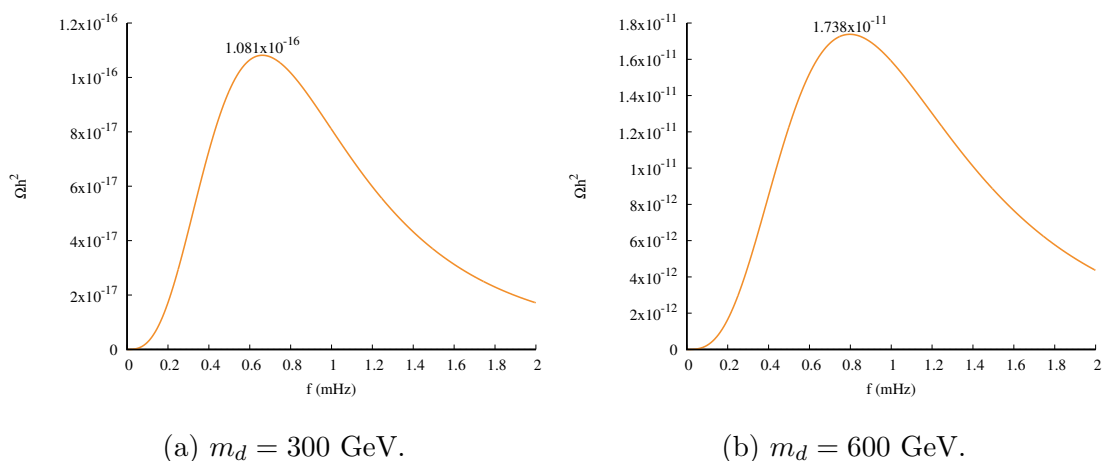


FIG. 4: Gravitational wave energy density.

The region from  $10^{-14}$  to  $10^{-11}$  is quite important, corresponding to  $400 \text{ GeV} \leq m_d < 550 \text{ GeV}$ , because it can be included in the residual sensitivities of the experiment. Specifically, based on sensitivity data of future detector, in Table III. DECIGO can pick up the signal of gravitational waves generated by the EWPT process in this model. The frequency domain for maximum gravitational wave energy density is  $0.4 - 1.2 \text{ mHz}$  which lies within the detection range of LISA, DECIGO and BBO.

TABLE III: Sensitivity of proposed GW

$f[mHz]$	$\Omega h^2$	Observatory	Ref.
0.02 – 0.12	$[0.02 - 1] \times 10^{-10}$	LISA	Refs.[57–59]
	$[0.5 - 8] \times 10^{-14}$	DECIGO	Refs.[57–59]
	—	BBO	Refs.[57–59]

#### IV. CONCLUSION AND DISCUSSION

$m_d$	$v_c$	$T_c$	$S$	$E$ [GeV]	$E_0$ [GeV]	$E_0/v_0$	$E_c/v_c$	$\frac{ E_0/v_0 - E_c/v_c }{E_0/v_0}$	Decoupling	Daisy loops
300	107.492	136.162	0.789	7658.14	9106.11	37.01	71.24	92.48%	57.09	with
	98.2028	146.281	0.671	7636.04			77.75	110%	53.57	without
350	133.417	129.726	1.028	7751.48	9094.9	36.98	58.1	57.11%	59.78	with
	128.617	138.449	0.928	7727.12			60.07	62.43%	56.17	without
400	160.455	122.702	1.307	7905.02	9079.14	36.91	49.26	33.45%	63.69	with
	158.371	130.329	1.215	7888.4			49.8	34.92%	60.04	without
450	190.502	115.103	1.655	8113.7	9055.43	36.81	42.59	15.7%	69.02	with
	189.376	121.835	1.554	8106.3			42.8	16.27%	65.27	without
500	229.877	108.027	2.127	8392.06	9020.63	36.67	36.5	0.4%	75.42	with
	227.515	113.854	1.998	8384.29			36.85	0.49%	71.59	without
550	287.102	106.276	2.701	8792.76	8970.03	36.46	30.61	16%	79.74	with
	281.168	110.832	2.536	8769.76			31.19	14.45%	76.34	without
600	348.246	114.415	3.043	9264.72	8895.83	36.16	26.6	26.43%	77.64	with
	339.772	117.85	2.883	9229			27.16	24.89%	75.16	without

TABLE IV: Results with the decoupling condition and the scaling law.

The scaling sphaleron law [60–62], the assumption to calculate the sphaleron energy at high temperature knowing it is at 0K ( $E_0$  or  $E(0K)$ ). It assumes that  $E(0K) = \frac{v}{v_T} E(T)$ . However, as the data in Table IV, this law is not exact. This is because  $v_{eff}(0k)$  and  $v_{eff}(T)$  are discontinuous when  $T \rightarrow 0$ .  $v_{eff}(T)$  is only valid for  $T \neq 0$ . This law can only be true in

the temperature range from  $T_N$  (the nucleation one) to  $T_c$ . Furthermore, from Table IV,  $E_0$  decreases very slowly,  $E(T)$  increases rapidly corresponding to  $300 \text{ GeV} \leq m_d \leq 600 \text{ GeV}$ . Because  $f(r), h(r)$  at 0K approach 1 more slowly than they do at a non-zero temperature. However, this law is accurate for  $m_d = 400 \text{ GeV}$  which may be the best value for Dilaton.

The decoupling condition [63–65], the important one, which is related to the sphaleron rate and the expansion rate of Universe,

$$\frac{E_{sph}(T)}{T} - 7\ln\left(\frac{v(T)}{T}\right) + \ln\left(\frac{T}{100\text{GeV}}\right) > 43. \quad (34)$$

In Table IV, the sphaleron energy at  $T_c$  fully satisfies the condition in Eq.(34). Although the right-hand side of Eq.(34) may be slightly changed, the values in the 10th column of Table IV are considerably larger than 43.

Finally, in the future, LISA, DECIDO and BBO can detect gravitational waves in the expected range. The GW of EWPT calculations could be a hint to indicate that there may be a contribution from the EWPT process in the detected wave spectrum. Additionally, the gravitational wave observations relevant to the early universe are summarized in Ref.[66]. Thus we have completely investigated the EWPT problem, calculating the Sphaleron energy and gravitational waves. The key conditions for concluding the Baryogenesis scenario.

## ACKNOWLEDGMENTS

This research is funded by University of Science, VNU-HCM under grant number T2024-10.

- 
- [1] I. Bars, C. Deliduman and D. Mimic, Phys. Rev. D **59**, 125004 (1999).
  - [2] I. Bars, Phys. Rev. D **62**, 046007 (2000).
  - [3] I. Bars, AIP conference proceedings **607**, 17 (2002).
  - [4] I. Bars, Class. and Quantum Grav. **18**, 3113-3130 (2001).
  - [5] I. Bars, Phys. Rev. D **74**, 085019 (2006).
  - [6] I. Bars and Y-C. Kuo, Phys. Rev. D **74** 085020 (2006).
  - [7] I. Bars , Phys.Rev.D **74**, 085019 (2006).

- [8] G. W. Anderson and L. J. Hall, Phys. Rev. D **45**, 2685-2698 (1992).
- [9] A. D. Sakharov, JETP Lett. **5**, 24 (1967).
- [10] M. Bastero-Gil, C. Hugonie, S. F. King, D. P. Roy, and S. Vempati, Phys. Lett. B **489**, 359 (2000).
- [11] A. Menon, D. E. Morrissey, and C. E. M. Wagner, Phys. Rev. D **70**, 035005 (2004).
- [12] S. W. Ham, S. K. Oh, C. M. Kim, E. J. Yoo, and D. Son, Phys. Rev. D **70**, 075001 (2004).
- [13] J. M. Cline, G. Laporte, H. Yamashita, S. Kraml, JHEP **0907**, 040 (2009).
- [14] S. Kanemura, Y. Okada, E. Senaha, Phys. Lett. B **606**, 361-366 (2005).
- [15] G. C. Dorsch, S. J. Huber, J. M. No, JHEP **10**, 029 (2013).
- [16] S. W. Ham, S-A Shim, and S. K. Oh, Phys. Rev. D **81**, 055015 (2010).
- [17] V. Q. Phong, V. T. Van, and H. N. Long, Phys. Rev. D **88**, 096009 (2013).
- [18] V. Q. Phong, H. N. Long, V. T. Van, N. C. Thanh, Phys. Rev. D **90**, 085019 (2014).
- [19] V. Q. Phong, H. N. Long, V. T. Van, L. H. Minh, Eur. Phys. J. C **75**, 342 (2015).
- [20] J. Sá Borges, R. O. Ramos, Eur. Phys. J. C **76**, 344 (2016).
- [21] S. Kanemura, E. Senaha, T. Shindou and T. Yamada, JHEP **1305**, 066 (2013).
- [22] D. J. H. Chung and A. J. Long, Phys. Rev. D **81**, 123531 (2010) .
- [23] G. Barenboim and N. Rius, Phys. Rev. D **58**, 065010 (1998).
- [24] F. Pisano and V. Pleitez, Phys. Rev. D **46**, 410 (1992).
- [25] P. H. Frampton, Phys. Rev. Lett. **69**, 2889 (1992).
- [26] R. Foot *et al*, Phys. Rev. D **47**, 4158 (1993).
- [27] M. Singer, J. W. F. Valle and J. Schechter, Phys. Rev. D **22**, 738 (1980).
- [28] R. Foot, H. N. Long and Tuan A. Tran, Phys. Rev. D **50**, R34 (1994).
- [29] J. C. Montero, F. Pisano and V. Pleitez, Phys. Rev. D **47**, 2918 (1993).
- [30] H. N. Long, Phys. Rev. D **54**, 4691 (1996).
- [31] H. N. Long, Phys. Rev. D **53**, 437 (1996).
- [32] A. J. Buras, F. De Fazio, J. Girrbach and M. V. Carlucci, JHEP **1302**, 023 (2013).
- [33] H. H. Patel, M. J. Ramsey-Musolf, JHEP **1107**, 029 (2011).
- [34] G. W. Anderson and L. J. Hall, Phys. Rev. D **45**, 2685 (1992).
- [35] Vo Quoc Phong and Dam Quang Nam, International Journal of Modern Physics A, Vol. 38, Nos. 29 & 30 (2023) 2350159.
- [36] I. Bars, P. Steinhardt, Neil Turok, Phys. Rev. D **89**, 043515 (2014).

- [37] S. Coleman and E. Weiberg, *Phys. Rev. D* **7**, 1888 (1973).
- [38] R. Jackiw, *Phys. Rev. D* **9**, 1686 (1974).
- [39] L. Dolan and R. Jackiw, *Phys. Rev. D* **9**, 3320 (1974).
- [40] G. W. Anderson and L. J. Hall, *Phys. Rev. D* **45**, 2685 (1992).
- [41] M. E. Carrington, *Phys. Rev. D* **45**, 2933 (1992).
- [42] David Curtin, Patrick Meade, Harikrishnan Ramani, *Eur. Phys. J. C* **78**, 787 (2018).
- [43] A. Katz and M. Perelstein, *JHEP* **07** 108 (2014).
- [44] Xucheng Gan, Andrew J. Long, and Lian-Tao Wang, *Phys. Rev. D* **96**, 115018 (2017).
- [45] Chiara Caprini, etc. , *JCAP***04**, 001 (2016).
- [46] A. Kosowsky, M. S. Turner, and R. Watkins, *Phys. Rev. D* **45**, 4514 (1992).
- [47] A. Kosowsky, M. S. Turner, and R. Watkins, *Phys. Rev. Lett.* **69**, 2026 (1992).
- [48] A. Kosowsky and M. S. Turner, *Phys. Rev. D* **47**, 4372 (1993).
- [49] S. J. Huber and T. Konstandin, *JCAP* **08099**, 022 (2008).
- [50] R. Jinno and M. Takimoto, *Phys. Rev. D* **95**, 024009 (2017).
- [51] R. Jinno and M. Takimoto, *JCAP* **1901**, 060 (2019).
- [52] R. Zhou, L. Bian and H-K Guo, *Phys. Rev. D* **101**, 091903 (2020).
- [53] Vo Quoc Phong, Nguyen Chi Thao, and Hoang Ngoc Long, *Eur. Phys. J. C* **82**, 1005 (2022).
- [54] L. Leitao, A. Megevand, A. D. Sanchez, *JCAP* **10**, 024 (2012).
- [55] M. S Tuner and S. Wilzek, *Phy. Rev.* **65**, 3080 (1990).
- [56] Christophe Grojean, G. Servant, *Phys. Rev. D* **75**, 043507 (2007).
- [57] S.V. Demidov, D. S. Gorbunov, D. V. Kirpichnikov, *Physics Letters B* **779**, 191 (2018).
- [58] Hideaki Kudoh, Atsushi Taruya, Takashi Hiramatsu, and Yoshiaki Himemoto, *Phys. Rev. D* **73**, 064006 (2006).
- [59] Eric Thrane1 and Joseph D. Romano, *Phys. Rev. D* **88**, 124032 (2013).
- [60] Yves Brihaye and Jutta Kunz *Phys. Rev. D* **48**, 3884 (1993).
- [61] Sylvie Braibant, Yves Brihaye, Jutta Kunz, *Int.J.Mod.Phys. A* **8**, 5563-5574 (1993).
- [62] Ruiyu Zhou, Ligong Bian, and Huai-Ke Guo, *Phys. Rev. D* **101**, 091903(R) (2020).
- [63] K. Funakubo and E. Senaha, *Phys. Rev. D* **79**, 115024 (2009).
- [64] M. Dvornikov and V. B. Semikoz, *Phys. Rev. D* **87**, 025023 (2013).
- [65] T. M. Gould and I. Z. Rothstein, *Phys. Rev. D* **48**, 5917 (1993).
- [66] Rishav Roshan, Graham White, arXiv:2401.04388.